

Table 1 Relationship between clinicopathological features and expression levels of *MYBL2* in 37 hepatocellular carcinomas (HCC)

	<i>MYBL2</i>		P*
	Low (≤ median) (n = 19)	High (> median) (n = 18)	
Age			
<65	6	13	0.013
≥65	13	5	
Sex			
Male	13	14	0.522
Female	6	4	
Tumor size			
<5 cm	8	11	0.248
≥5 cm	11	7	
Tumor differentiation			
Well	3	2	0.403
Moderate	11	14	
Poorly	5	2	
Stage			
I, II, III	16	12	0.214
IV	3	6	
HBV infection status			
Positive	2	6	0.158
Negative	16	10	
Unknown	1	2	
HCV infection status			
Positive	15	11	0.491
Negative	3	5	
Unknown	1	2	
Background liver tissue			
Normal	1	1	0.492
Chronic hepatitis	15	11	
Liver Cirrhosis	1	4	
Unknown	2	2	

* χ^2 test.

next examined the available data from 37 HCC patients, whose tumors were divided into high- and low-expression groups based on where they fell relative to the median of level of *MYBL2* mRNA expression (Table 1). High expression of *MYBL2* was significantly associated with samples from patients less than 65 years old as compared with samples from patients 65 and older. However, we observed no significant link with any other parameter that was examined, including the sex of the patient, the size, degree of differentiation, or stage of the tumor, HBV or HCV infection, or features of non-tumorous liver samples from these patients.

Amplification of *MYBL2* in HCC

Amplification of chromosomal DNA is one of several mechanisms capable of activating genes, a phenomenon that contributes to the development and progression of cancers. *MYBL2* is located at 20q13, where a gain in DNA copy number is frequently observed in various tumors,¹⁹ including HCC.²⁰ Based on this observation, we decided to determine the *MYBL2* copy number in DNA derived from 21 liver cancer cell lines (20 HCC cells and the hepatoblastoma line HepG2) using real-time quantitative PCR. Copy number changes were counted as gains if the results for a given cell line exceeded the mean plus twice the standard deviation of the levels of *MYBL2* observed in genomic DNA derived from four samples of peripheral blood lymphocytes (i.e. from normal cells). *MYBL2* exhibited copy-number gain in 19 of the 20 lines (Fig. 3A). We then used FISH to more directly test copy-number gain of *MYBL2* in these cell lines. In JHH-5 cells, a representative example, the number of FISH signals was higher than normal (i.e. seven signals were detected in single cells; Fig. 3B). In addition, to ask if *MYBL2* was amplified in primary tumors, we examined 66 primary HCCs for a gain in copy number. Copy-number gain for *MYBL2* was observed in 36 of the 66 tumors (55%; Fig. 3C). These findings suggested that copy-number gain of *MYBL2* acts synergistically with transcriptional activity of E2F1 to upregulate *MYBL2* expression in HCCs.

B-Myb downstream genes

To explore B-Myb-inducible genes in HCC, we analyzed eight genes previously reported to be downstream targets of B-Myb: *CDC2*;²¹ *CCNA2*;²² *TOP2A* (which encodes DNA topoisomerase II α);²³ *FGF4* (fibroblast growth factor 4);²⁴ *POLA* (DNA polymerase α);²⁵ *CCND1* (cyclin D1);²¹ *CLU* (clusterin/Apo);²⁶ and *BCL2* (*BCL-2*).²⁷ Of these, *CDC2*, *CCNA2*, *TOP2A*, *FGF4*, *POLA*, and *CCND1* have been implicated in progression of cell cycle, and *CLU* and *BCL2* appear to be involved in anti-apoptotic activity. We knocked down expression of *MYBL2* via siRNA in JHH-5 cells (Fig. 4A). Upon siRNA-mediated knockdown of *MYBL2*, we observed reduced expression of only *CDC2*, *CCNA2*, and *TOP2A* among the eight candidate genes examined (Fig. 4A). These three genes (*CDC2*, *CCNA2*, and *TOP2A*) were significantly over-expressed in 22 primary HCC tumors as compared with their counterpart non-tumorous tissues (Fig. 4B); that is, *CDC2* was over-expressed in 21 HCC tumors (95%); *CCNA2* in 20 (91%); and *TOP2A* in 19 (86%). Moreover, expression levels of *MYBL2*

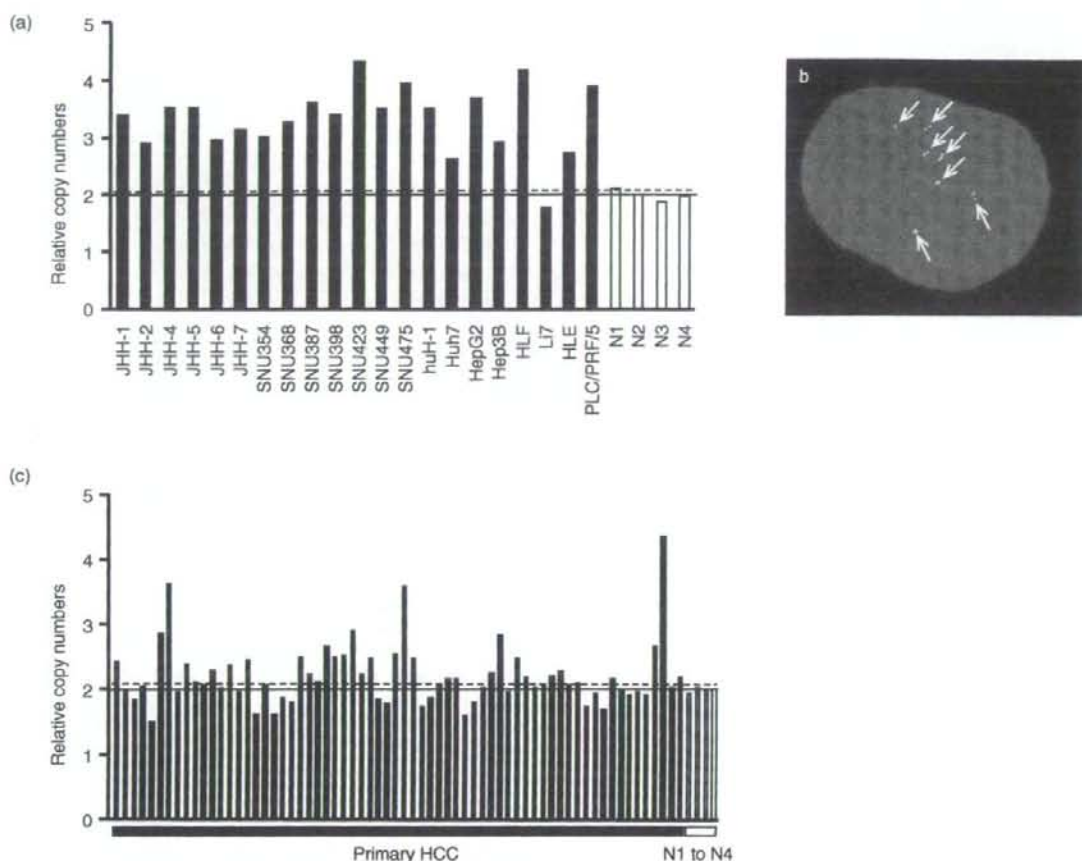


Figure 3 Amplification of *MYBL2* in hepatocellular carcinoma (HCC). (A) Relative copy number of *MYBL2* determined by real-time quantitative PCR in 21 HCC cell lines and normal peripheral lymphocytes (N1 to N4). Results are presented as the ratio between *MYBL2* and a LINE-1 control, and were normalized such that the average ratio in four normal DNAs (N1 to N4) is 2 (solid horizontal line). The mean + 2 × SD of normal lymphocytes (dotted line) was used as the cut-off for a copy-number gain. (B) Representative image of interphase FISH for *MYBL2* in JHH-5 cells. In this case, seven twin-spot FISH signals can be observed. (C) Relative copy number of *MYBL2* in 66 primary HCC tumors determined as in (A). Values were normalized such that the average copy number of *MYBL2* in genomic DNA derived from four normal lymphocytes is 2 (solid horizontal line). The mean + 2 × SD of normal lymphocytes (dotted line) was used as the cut-off for a copy-number gain.

significantly correlated with those of *CDC2*, *CCNA2*, and *TOP2A* in 22 primary HCCs (Fig. 4C). These results suggest that *CDC2*, *CCNA2*, and *TOP2A* are probable transcriptional targets of B-Myb in HCC.

DISCUSSION

IN THE PRESENT study, we examined expression of *E2F1* and candidate *E2F1* target genes in primary HCCs. Our results show that both *E2F1* and *MYBL2* are

over-expressed in primary HCCs (Figs 1,2B,C) and that there is a significant correlation between expression of *E2F1* and *MYBL2* (Fig. 2D). RNAi-mediated reduction of *E2F1* in HCC-derived cells inhibits expression of *MYBL2* (Fig. 2A). These findings suggest that *MYBL2* may be a transcriptional target of *E2F1*, which could explain the upregulation of *MYBL2* we observed in HCC. Furthermore, a gain in *MYBL2* copy-number was frequently observed in both HCC cell lines and primary HCC tumors (Fig. 3). Thus, in addition to

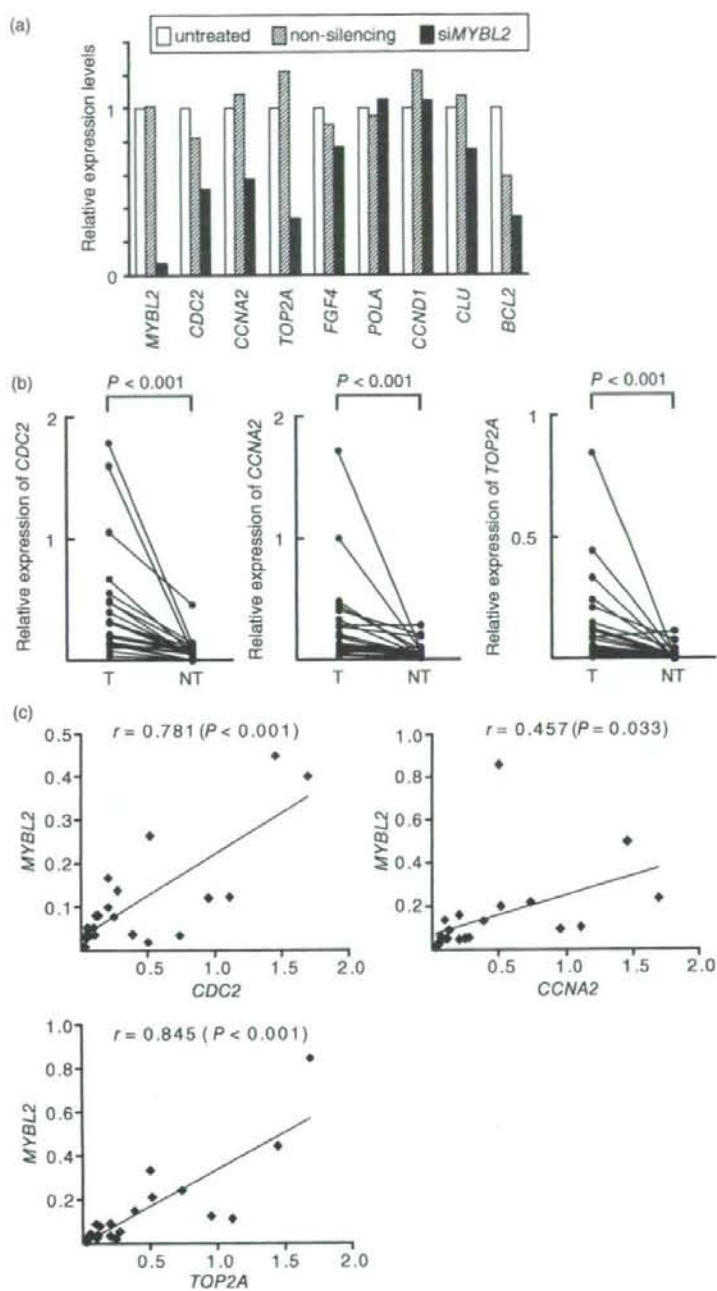


Figure 4 *CDC2*, *CCNA2*, and *TOP2A* are probable transcriptional targets of *MYBL2* in hepatocellular carcinoma (HCC). (A) siRNA-mediated knockdown of *MYBL2* in HCC cell lines. JHH-5 cells were treated with 5 nM siRNA targeting *MYBL2* (si*MYBL2*) or control siRNA (non-silencing), and harvested 48 h after transfection. Untreated cells were maintained under identical experimental conditions. Relative expression of *MYBL2* and putative downstream genes were evaluated by real-time quantitative RT-PCR. Results are presented as the ratio between expression of each gene and a reference (*GAPDH*) to correct for variation in the amount of RNA. Relative expression levels were normalized such that the ratio in untreated cells is 1. (B) Relative expression of *CDC2*, *CCNA2*, and *TOP2A* in paired tumor (T) and non-tumor (NT) tissues from 22 patients as determined by real-time quantitative RT-PCR. (C) Correlation between expression of *MYBL2* and that of *CDC2*, *CCNA2*, or *TOP2A* in 22 primary HCC tumors. Pearson's correlation coefficient analysis revealed that there was a significant correlation between the level of expression of *MYBL2* and that of each of the three genes.

transcriptional activation of *MYBL2* by E2F1, expression of *MYBL2* may also be upregulated in HCC as a result of amplification of the *MYBL2*-containing genomic region in these cells.

Our results are consistent with earlier research. *MYBL2* is frequently amplified in a variety of tumor types, including breast,²⁸ ovarian,²⁹ melanoma,³⁰ and HCC.³¹ Moreover, *MYBL2* is amplified and over-expressed in breast cancer cell lines.³² *MYBL2* is over-expressed in prostate metastases relative to localized tumors.³³ Elevated expression of *MYBL2* is also observed in advanced neuroblastoma and correlates with a poor prognosis.³⁴ Although the direct role of B-Myb in cancers is not yet fully established, these lines of evidence, together with ours, indicate that B-Myb has oncogenic potential.

We also looked at the relationship between expression levels of *MYBL2* in primary HCCs and clinicopathological parameters (Table 1). With the exception of the age of the patient, no parameter tested, including tumor size, differentiation or stage, correlated with *MYBL2* expression. This may suggest that *MYBL2* is upregulated in early stages of HCC formation.

We next examined transcriptional targets of B-Myb in HCC. Among the eight candidate genes examined, only *CDC2*, *CCNA2*, and *TOP2A* were suppressed at the mRNA level following siRNA-mediated knockdown of *MYBL2* (Fig. 4A). Correspondingly, these three genes are significantly over-expressed in primary HCC tumors (Fig. 4B) and expression of the three genes correlates with *MYBL2* expression (Fig. 4C). These results suggest that *CDC2*, *CCNA2*, and *TOP2A* are downstream targets of B-Myb. Interestingly, Cyclin A2, which is encoded by *CCNA2*, forms a complex with *CDC2*, whose activity peaks at the G2/M transition of cell cycle, and *CDC2*-cyclin A2 kinase activity is required to enter M phase. Our results are consistent with the recent findings that B-Myb, together with E2F1, regulates expression of genes required for the G2/M phase of the cell cycle, such as *CDC2*, cyclin A2, and cyclin B1.²²

We found that si-RNA-mediated reduction of *E2F1* inhibited expression of *MYBL2*, but not *CCNA2* (Fig. 2A). However, si-RNA-mediated knockdown of *MYBL2* inhibited expression of *CCNA2* (Fig. 4A). It is unclear why reduction of *E2F1* did not lead to a decrease in expression of *CCNA2* through a decrease in the expression of *MYBL2*. There might be a time lag between suppression of *MYBL2* and *CCNA2* expression following si-RNA-mediated knockdown of *E2F1*.

Topoisomerase II α , which is encoded by *TOP2A*, forms breaks in double-stranded DNA, allowing strands to separate during replication. Cyclin A2, *CDC2*, and topoisomerase II α are all essential for cell cycle progression. Thus, these genes seem reasonable target for B-Myb regulation.

We have shown that *E2F1* is over-expressed in primary HCC tumors and that *MYBL2* expression is also up-regulated in HCCs, suggesting that *MYBL2* is a transcriptional target of E2F1. Frequent amplification of *MYBL2* in HCCs is likely to be an additional mechanism leading to *MYBL2* over-expression. Further, the *CDC2*, *CCNA2*, and *TOP2A* genes may be transcriptional targets of B-Myb. Our results suggest that B-Myb may play an important role in initiation or progression (or both) of HCC and thus, may represent an optimal target for development of novel therapies for this widespread tumor type.

ACKNOWLEDGMENT

THIS WORK WAS supported by Grants-in-Aid for Scientific Research from the Japan Society for the Program of Science (KY).

REFERENCES

- 1 El-serag HB. Hepatocellular carcinoma: an epidemiologic view. *J Clin Gastroenterol* 2002; 35: S72–8.
- 2 Johnson DG, Degregori J. Putting the oncogenic and tumor suppressive activities of E2F into context. *Curr Mol Med* 2006; 6: 731–8.

- 3 DeGregori J, Johnson DG. Distinct and overlapping roles for E2F family members in transcription, proliferation and apoptosis. *Curr Mol Med* 2006; 6: 739–48.
- 4 Yasui K, Arai S, Zhao C *et al.* TFDPI, CUL4A, and CDC16 identified as targets for amplification at 13q34 in hepatocellular carcinomas. *Hepatology* 2002; 35: 1476–84.
- 5 Shinomiya T, Mori T, Ariyama Y *et al.* Comparative genomic hybridization of squamous cell carcinoma of the esophagus: the possible involvement of the DP1 gene in the 13q34 amplicon. *Genes Chromosomes Cancer* 1999; 24: 337–44.
- 6 Yasui K, Okamoto H, Arai S, Inazawa J. Association of over-expressed TFDPI with progression of hepatocellular carcinomas. *J Hum Genet* 2003; 48: 609–13.
- 7 Bell LA, Ryan KM. Life and death decisions by E2F-1. *Cell Death Differ* 2004; 11: 137–42.
- 8 Sala A. B-MYB, a transcription factor implicated in regulating cell cycle, apoptosis and cancer. *Eur J Cancer* 2005; 41: 2479–84.
- 9 Joaquin M, Watson RJ. Cell cycle regulation by the B-Myb transcription factor. *Cell Mol Life Sci* 2003; 60: 2389–401.
- 10 DeGregori J, Kowalik T, Nevins JR. Cellular targets for activation by the E2F1 transcription factor include DNA synthesis- and G1/S-regulatory genes. *Mol Cell Biol* 1995; 15: 4215–24.
- 11 Tanaka Y, Patestos NP, Maekawa T, Ishii S. B-myb is required for inner cell mass formation at an early stage of development. *J Biol Chem* 1999; 274: 28067–70.
- 12 Dor I, Namba M, Sato J. Establishment and some biological characteristics of human hepatoma cell lines. *Gann* 1975; 66: 385–92.
- 13 Hirohashi S, Shimamoto Y, Kameya T *et al.* Production of alpha-fetoprotein and normal serum proteins by xenotransplanted human hepatomas in relation to their growth and morphology. *Cancer Res* 1979; 39: 1819–28.
- 14 Park JG, Lee JH, Kang MS *et al.* Characterization of cell lines established from human hepatocellular carcinoma. *Int J Cancer* 1995; 62: 276–82.
- 15 Fujise K, Nagamori S, Hasumura S *et al.* Integration of hepatitis B virus DNA into cells of six established human hepatocellular carcinoma cell lines. *Hepato-gastroenterology* 1990; 37: 457–60.
- 16 Huh N, Utakoji T. Production of HBs-antigen by two new human hepatoma cell lines and its enhancement by dexamethasone. *Gann* 1981; 72: 178–9.
- 17 Minamiya Y, Matsuzaki I, Sageshima M *et al.* Expression of tissue factor mRNA and invasion of blood vessels by tumor cells in non-small cell lung cancer. *Surg Today* 2004; 34: 1–5.
- 18 Zhao X, Li C, Paez JG *et al.* An integrated view of copy number and allelic alterations in the cancer genome using single nucleotide polymorphism arrays. *Cancer Res* 2004; 64: 3060–71.
- 19 Knuutila S, Björkqvist AM, Autio K *et al.* DNA copy number amplifications in human neoplasms: review of comparative genomic hybridization studies. *Am J Pathol* 2000; 157: 689.
- 20 Okamoto H, Yasui K, Zhao C, Arai S, Inazawa J. PTK2 and EIF3S3 genes may be amplification targets at 8q23–q24 and are associated with large hepatocellular carcinomas. *Hepatology* 2003; 38: 1242–9.
- 21 Sala A, Calabretta B. Regulation of BALB/c 3T3 fibroblast proliferation by B-myb is accompanied by selective activation of cdc2 and cyclin D1 expression. *Proc Natl Acad Sci USA* 1992; 89: 10415–19.
- 22 Zhu W, Giangrande PH, Nevins JR. E2Fs link the control of G1/S and G2/M transcription. *EMBO J* 2004; 23: 4615–26.
- 23 Brandt TL, Fraser DJ, Leal S, Halandras PM, Kroll AR, Kroll DJ. c-Myb trans-activates the human DNA topoisomerase II alpha gene promoter. *J Biol Chem* 1997; 272: 6278–84.
- 24 Johnson LR, Johnson TK, Desler M *et al.* Effects of B-Myb on gene transcription: phosphorylation-dependent activity and acetylation by p300. *J Biol Chem* 2002; 277: 4088–97.
- 25 Watson RJ, Robinson C, Lam EW. Transcription regulation by murine B-myb is distinct from that by c-myb. *Nucleic Acids Res* 1993; 21: 267–72.
- 26 Cervellera M, Raschella G, Santilli G *et al.* Direct transactivation of the anti-apoptotic gene apolipoprotein J (clusterin) by B-MYB. *J Biol Chem* 2000; 275: 21055–60.
- 27 Grassilli E, Salomoni P, Perrotti D, Franceschi C, Calabretta B. Resistance to apoptosis in CILL-2 cells overexpressing B-Myb is associated with B-Myb-dependent bcl-2 induction. *Cancer Res* 1999; 59: 2451–6.
- 28 Ginestier C, Cervera N, Finetti P *et al.* Prognosis and gene expression profiling of 20q13-amplified breast cancers. *Clin Cancer Res* 2006; 12: 4533–44.
- 29 Tanner MM, Grenman S, Koul A *et al.* Frequent amplification of chromosomal region 20q12–q13 in ovarian cancer. *Clin Cancer Res* 2000; 6: 1833–9.
- 30 Koynova DK, Jordanova ES, Milev AD *et al.* Gene-specific fluorescence in-situ hybridization analysis on tissue microarray to refine the region of chromosome 20q amplification in melanoma. *Melanoma Res* 2007; 17: 37–41.
- 31 Zondervan PE, Wink J, Alers JC *et al.* Molecular cytogenetic evaluation of virus-associated and non-viral hepatocellular carcinoma: analysis of 26 carcinomas and 12 concurrent dysplasias. *J Pathol* 2000; 192: 207–15.
- 32 Forozaan F, Mahlamäki EH, Monni O *et al.* Comparative genomic hybridization analysis of 38 breast cancer cell lines: a basis for interpreting complementary DNA microarray data. *Cancer Res* 2000; 60: 4519–25.
- 33 Bar-Shira A, Pinthus JH, Rozovsky U *et al.* Multiple genes in human 20q13 chromosomal region are involved in an advanced prostate cancer xenograft. *Cancer Res* 2002; 62: 6803–7.

- 34 Raschellà G, Cesi V, Amendola R *et al.* Expression of B-myb in neuroblastoma tumors is a poor prognostic factor independent from MYCN amplification. *Cancer Res* 1999; 59: 3365–8.

Table S1. Primer sequences used for RT-PCR assays.
Table S2. Primer sequences used for genomic PCR assays.

This material is available as part of the online article from <http://www.blackwell-synergy.com>

SUPPLEMENTARY MATERIAL

THE FOLLOWING SUPPLEMENTARY material is available for this article online:

CREB3L4, *INTS3*, and *SNAPAP* are targets for the 1q21 amplicon frequently detected in hepatocellular carcinoma

Yoshikazu Inagaki^a, Kohichiroh Yasui^{a,*}, Mio Endo^a, Tomoaki Nakajima^a, Keika Zen^a, Kazuhiro Tsuji^a, Masahito Minami^a, Shinji Tanaka^b, Masafumi Taniwaki^c, Yoshito Itoh^a, Shigeki Arii^b, Takeshi Okanoue^a

^aMolecular Gastroenterology and Hepatology, Graduate School of Medical Science, Kyoto Prefectural University of Medicine, 465 Kajicho Kamigyo-ku, Kyoto 602-8566, Japan

^bDepartment of Hepato-Biliary-Pancreatic Surgery, Tokyo Medical and Dental University, Tokyo, Japan

^cMolecular Hematology and Oncology, Graduate School of Medical Science, Kyoto Prefectural University of Medicine, Kyoto, Japan

Received 10 August 2007; accepted 25 September 2007

Abstract

High-density single nucleotide polymorphism (SNP) array analysis revealed novel amplification at 1q21 in cell lines derived from hepatocellular carcinomas (HCCs). Fluorescence in situ hybridization and real-time quantitative polymerase chain reaction studies verified amplification at 1q21. An increase in copy number at the region was detected in 32 of the 36 primary HCC tumors (89%). To identify the targets for amplification, we examined 19 HCC cell lines for expression levels of all 26 genes located within the 700-kb amplified region. Five genes were overexpressed in cell lines with amplification at 1q21. Among these, *CREB3L4* (cAMP responsive element binding protein 3-like 4), *INTS3* (integrator complex subunit 3), and *SNAPAP* (SNAP-associated protein) were significantly overexpressed in tumors from 18 HCC patients, compared with counterpart nontumorous tissues. The findings suggest that *CREB3L4*, *INTS3*, and *SNAPAP* are probable targets for the amplification mechanism and may therefore be involved, together or separately, in the development or progression of HCCs. © 2008 Elsevier Inc. All rights reserved.

1. Introduction

Amplification of DNA in certain chromosome regions plays a crucial role in the development and progression of human malignancies, specifically when proto-oncogenic target genes within those amplicons are overexpressed. Oncogenes that are often amplified in cancers include *MYC*, *ERBB2*, and *CCND1*. The initial approach to genome-wide detection of copy number aberrations in cancers was comparative genomic hybridization (CGH) [1]. Using CGH analyses, we detected novel regions of amplification in various types of tumor. Within these amplicons, we identified a number of additional proto-oncogenes that may be upregulated by DNA amplification [2–6]. CGH has limited resolution (5–10 Mb), however, in that it detects segmental copy number changes on metaphase chromosomes [1].

The recent introduction of high-density oligonucleotide microarrays designed for typing of single nucleotide polymorphisms (SNPs) allows for high-resolution mapping of

chromosomal amplifications, deletions, and loss of heterozygosity [7–11]. The GeneChip Mapping 100K array set (Affymetrix, Santa Clara, CA) contains 116,204 SNP loci, with a mean intermarker distance of 23.6 kb, and enables detailed and genome-wide identification of DNA copy number changes [12–14].

In the present study, we identified novel, high-level amplification at 1q21 using the Affymetrix GeneChip Mapping 100K array analysis against a panel of cell lines derived from hepatocellular carcinoma (HCC). Worldwide, HCC is the fifth most common malignancy in men and the eighth most common in women [15]. Previous CGH studies of HCC, including ours [3], have revealed that the most frequent copy number gains occur on 1q (58–78%) [16–18]. Gains in 1q21–q23 were identified as a genomic event associated with the early development of HCC [19]. Recurrent gains at 1q21–q23 have been observed in not only HCC but also in tumors including squamous cell carcinomas of the head and neck, lung cancer, desmoid tumors, and sarcomas [20,21]. These findings suggest that 1q21 harbors one or more proto-oncogenes whose overexpression following amplification contributes to the initiation or

* Corresponding author. Tel.: +81-75-251-5519; fax: +81-75-251-0710.

E-mail address: yasui@koto.kpu-m.ac.jp (K. Yasui).

progression of HCC. We therefore performed molecular definition of the 1q21 amplicon. Three genes emerged as possible targets: *CREB3LA*, *INTS3*, and *SNAPAP*.

2. Materials and methods

2.1. Cell lines and tumor samples

A total of 19 HCC-derived cell lines were examined: HLE [22], HLF [22], PLC/PRF/5 [23], Li7 [24], Huh7 [25], Hep3B [26], SNU354 [27], SNU368 [27], SNU387 [27], SNU398 [27], SNU423 [27], SNU475 [27], JHH-1 [28], JHH-2 [28], JHH-4 [28], JHH-5 [28], JHH-6 [28], JHH-7 [28], and Huh-1 [29]. All cell lines were maintained in Dulbecco's modified Eagle's medium (DMEM) supplemented with 10% fetal bovine serum. We obtained 36 primary HCC tumors from patients undergoing surgery at the hospital of Tokyo Medical and Dental University and Kyoto University. Genomic DNA was isolated from all cell lines and primary tumors using the Puregene DNA isolation kit (Gentra Systems, Minneapolis, MN).

Informed consent and Ethics Committee approval were obtained before initiation of the study.

2.2. SNP assay

GeneChip Mapping 100K array set (Affymetrix, Santa Clara, CA) analyses were performed according to the

manufacturer's instructions. Briefly, 250 ng of genomic DNA was digested with a restriction enzyme (*Xba*I or *Hin*dIII), ligated to an adaptor, and amplified by polymerase chain reaction (PCR) [8,9,30]. Amplified products were fragmented, labeled by biotinylation, and hybridized to microarrays. Hybridization was detected by incubation with streptavidin–phycoerythrin conjugate, followed by scanning, and analysis was performed as described previously [30,31].

Copy number changes were calculated based on SNP hybridization signal intensity data from the experimental sample relative to intensity distributions derived from a reference set containing > 100 individuals using the Affymetrix Chromosome Copy Number Analysis Tool software and algorithm (CNAT version 2.0; <http://www.affymetrix.com/support/developer/tools/affytools.affy>) [32].

2.3. Real-time quantitative PCR

We quantified genomic DNA and mRNA using the real-time fluorescence detection method. Total RNA was obtained using Trizol reagent (Invitrogen, Carlsbad, CA). Residual genomic DNA was removed by incubating RNA samples with RNase-free DNase I (Takara Bio, Shiga, Japan) prior to reverse transcriptase PCR. Single-stranded complementary DNA (cDNA) was generated using SuperScript III reverse transcriptase (Invitrogen) according to the manufacturer's directions. Real-time quantitative PCR

Table 1
Primer sequences used for real-time quantitative polymerase chain reaction (PCR)

Gene	Forward primer	Reverse primer	PCR product size, bp
<i>S100A6</i>	5'-GAAGGAGCTGAAGGAGCTGA-3'	5'-CCCTTGAGGGCTTCATTGTA-3'	177
<i>S100A5</i>	5'-AGAGCTGTGTCTGGGGAGA-3'	5'-CCCTGGTCACTTGTGTCTCT-3'	166
<i>S100A4</i>	5'-GATGAGCAACTGGACAGCA-3'	5'-CTICCTGGGCTGCTTATCTG-3'	127
<i>S100A3</i>	5'-CGAGGTGGACTTTGTGGAGT-3'	5'-GGGCCTCCTAGTAAATGG-3'	244
<i>S100A2</i>	5'-CTCCTGGTCTGTCTCTGC-3'	5'-TCCCCCTTACTCAGCTTGA-3'	142
<i>S100A16</i>	5'-ATGTTCTCTGCCAAATTCCTG-3'	5'-GAGAGGTCTCTGCTGTCTG-3'	142
<i>S10014</i>	5'-CTGACCCCTCTGAGCTACG-3'	5'-CCAGAGGGAGTCTCAGTGC-3'	214
<i>S100A13</i>	5'-TCCAACTGGAACCTTGAACC-3'	5'-GATCTGGAAGTGGTGGAGA-3'	155
<i>S100A1</i>	5'-GGAGCCCTCATCAACGTGT-3'	5'-CAGCCACAAGCACCAGATAC-3'	215
<i>C1orf77</i>	5'-GGTGGTAGAGGTCGGGGTAT-3'	5'-GCATCCAGGTGCTCTTTGT-3'	167
<i>SNAPAP</i>	5'-AGGAACGACTGAGACGGCTA-3'	5'-GTAAATCCCGAATCCAGCA-3'	80
<i>ILF2</i>	5'-CGTGGAAAGCCTAAGAGCAC-3'	5'-GAAGATTGGTGGCACTGTT-3'	128
<i>NPR1</i>	5'-GCATTGAGCTGACACGAAAA-3'	5'-CCTTGACGATGTCATTGGTG-3'	219
<i>INTS3</i>	5'-GGTACGGGAAGCTGGTGAAGA-3'	5'-CTGCTCTTCAGGACCCACTC-3'	162
<i>SLC27A3</i>	5'-ATACCTGGGAGCGTTTTGTG-3'	5'-CCGCTGTCTGTGTAGTTGA-3'	104
<i>GATAD2B</i>	5'-TICTTTTCCCTCTGTGCTTT-3'	5'-GGCATCTCGTACCTCTGAGC-3'	221
<i>KIAA0476^a</i>	5'-CTATGGGCTGTGGTCTCTGT-3'	5'-TGCCCATAGTGTGAGCAGAG-3'	171
<i>CRTC2</i>	5'-TICAGTGCAGTCTCAGGTG-3'	5'-GCTGAATGCTCCAGATTCC-3'	145
<i>SLC39A1</i>	5'-GGATGGGGAAGACACTTGA-3'	5'-GAAATGGGGTAGGACCAACA-3'	159
<i>CREB3LA</i>	5'-GACCAGAAGCTGGGCTGAG-3'	5'-TGTTACGTCCTTGTGGGTCA-3'	77
<i>JTB</i>	5'-ACGTATTGTCCTGCTCACC-3'	5'-GCTGCTCACTGGGAATTAGC-3'	165
<i>RAB13</i>	5'-GAGCCATGGGCATATCCTA-3'	5'-CCTTCTGCACCTTCTCTTG-3'	162
<i>RPS27</i>	5'-CGCAAAGGATCTCCTTCATC-3'	5'-CGTTTGTGCATGGCTAAAGA-3'	148
<i>NUP210L</i>	5'-CTGTGAACAGAGGGCTGACA-3'	5'-GCTCAATGGCATGCTCTACA-3'	96
<i>TPM3</i>	5'-GGGTTTGAAGCTGTCTCTC-3'	5'-CCACAACCCAAAGCAAAGT-3'	137
<i>C1orf89</i>	5'-ATGCAGGACACCATGGTACA-3'	5'-TCCTGCTGGTACTGCTGATG-3'	113

^a The approved gene symbol for the *KIAA0476* gene is now *DENND4B* (<http://www.genenames.org>). For simplicity, the previous symbol is retained.

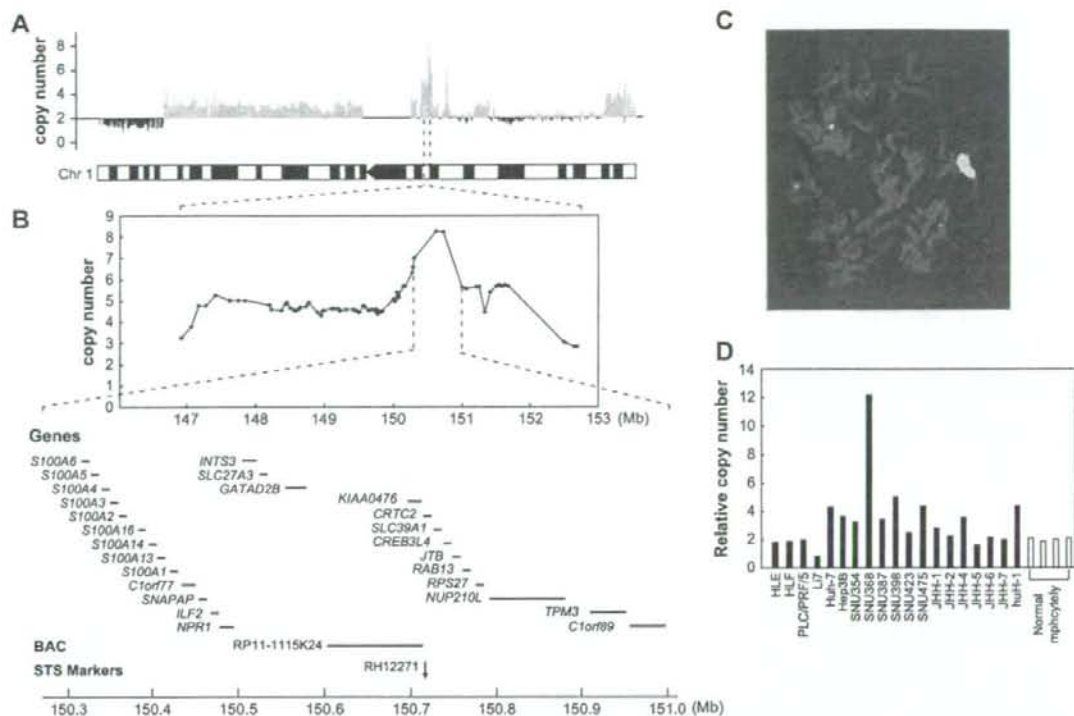


Fig. 1. Map of the amplicon at 1q21 in the hepatocellular carcinoma (HCC) cell line SNU368. (A) Copy number determined by SNP 100 K arrays (upper) and chromosome 1 cytoband map (lower) are shown. Copy number values were estimated using the Affymetrix CNAT chromosome copy number analysis tool. Green lines show copy number gains; red lines correspond to losses of genomic material. (B) Map of 1q21 amplicon. The graph represents the copy number determined by SNP arrays. The positions of the 26 genes within the amplicon, the bacterial artificial chromosome (BAC; RP11-1115K24) used as a probe for fluorescence in situ hybridization (FISH), and the STS marker (RH12271) used for real-time quantitative polymerase chain reaction (PCR) are shown, according to the UCSC genome database (<http://genome.ucsc.edu/>). (C) Representative FISH images using BAC RP11-1115K24 on metaphase chromosomes from SNU368 cells. The image shows strong homogeneously staining region signals on a marker chromosome. (D) Copy numbers at the STS marker locus RH12271 in 19 HCC cell lines and four normal peripheral blood lymphocytes, as measured by real-time quantitative PCR with reference to LINE-1 controls. Values are normalized such that the average copy number in genomic DNA derived from four normal lymphocytes has a value of 2.

experiments were performed with the LightCycler system using FastStart DNA Master Plus SYBR Green I (Roche Diagnostics, Penzberg, Germany) according to the manufacturer's protocol. Primers used for PCR (listed in Table 1) were designed using Primer3 version 0.4 (http://frodo.wi.mit.edu/cgi-bin/primer3/primer3_www.cgi) on the basis of sequence data obtained from the U.S. National Center for Biotechnology Information Entrez Gene database (<http://www.ncbi.nlm.nih.gov/>). GAPDH [33] and long interspersed nuclear element 1 (LINE-1) [9] were used as endogenous controls for mRNA and genomic DNA levels, respectively.

2.4. Fluorescence in situ hybridization

Fluorescence in situ hybridization (FISH) experiments were performed using bacterial artificial chromosome (BAC; RP11-1115K24) as a probe, as described previously [2]. Briefly, the probe was labeled with biotin-16-dUTP

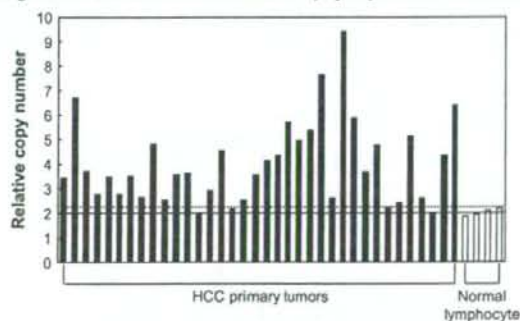


Fig. 2. Copy number gain at 1q21 in primary HCC tumors. Copy number at the STS marker locus RH12271 in 36 primary HCC tumors and four normal peripheral blood lymphocytes were determined by real-time quantitative PCR with reference to LINE-1 controls. Values are normalized such that the average copy number in genomic DNA derived from four normal lymphocytes has a value of 2 (solid horizontal line). The mean + 2 × SD of normal lymphocytes was used to determine the cutoff value for copy number gain (dotted horizontal line).

(Roche Diagnostics) by nick translation and was hybridized to metaphase chromosomes. Hybridization signals for biotin-labeled probes were detected using avidin–fluorescein (Roche Diagnostics).

3. Results

3.1. Detection of 1q21 amplicon in HCC cell lines by SNP array analysis

In the course of investigating DNA copy number aberrations in HCC cell lines by high-density SNP microarray (Affymetrix GeneChip Mapping 100K array), we found that SNU368 cells exhibited high-level amplification at 1q21 (Figs. 1A, 1B). The extent of this amplicon was estimated to be 700 kb (between Affymetrix SNP_A-1737869 and SNP_A-1662365). FISH analysis in SNU368 cells, using BAC RP11-1115K24 as a probe (Fig. 1B), revealed

a strong homogeneously staining region (HSR), indicating high-level amplification (Fig. 1C). Furthermore, we determined gene dosage at the STS marker RH12271 (Fig. 1B) locus present within the amplicon by real-time quantitative PCR using DNA derived from 19 HCC cell lines. Amplification at the locus was observed in SNU368 cells (Fig. 1D). These findings confirmed amplification at 1q21 in SNU368 cells.

3.2. Amplification of 1q21 locus in primary HCC tumors

To determine whether the 1q21 region was amplified in primary tumors, we examined copy numbers at STS marker RH12271 in 36 primary HCCs by real-time quantitative PCR. Copy number changes were rated as gains if they exceeded the mean plus 2 standard deviations of the levels in normal genomic DNA derived from four peripheral blood lymphocytes. The locus was amplified in 32 of the 36 tumors (89%) (Fig. 2).

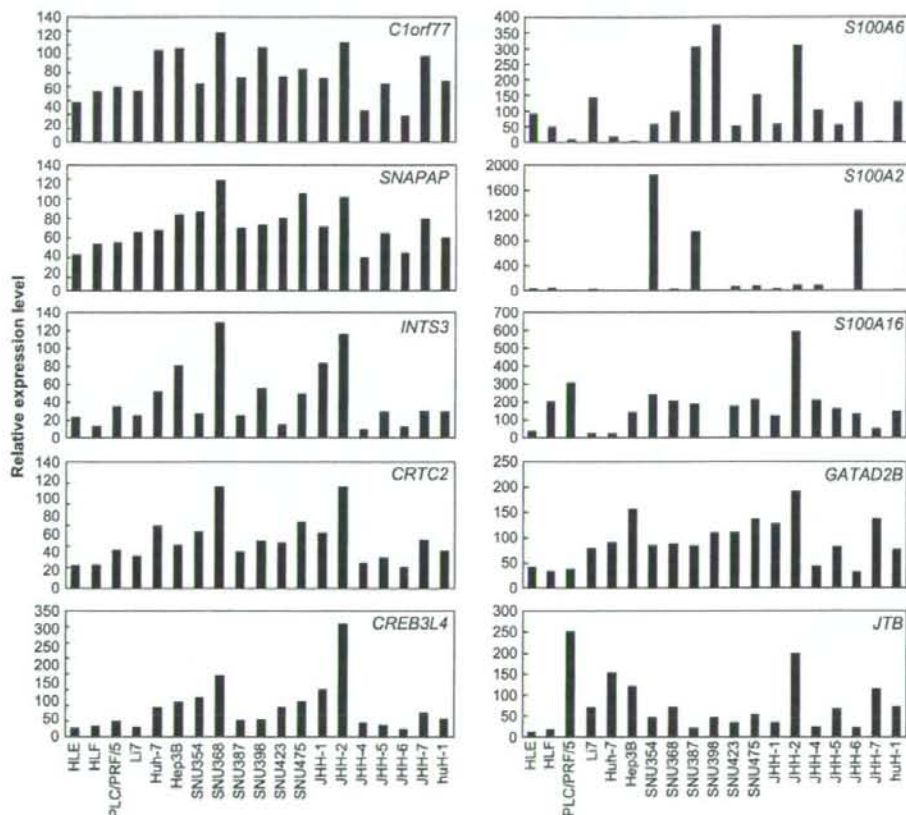


Fig. 3. Relative expression levels of 10 representative genes within the 1q21 amplicon in panel of 19 HCC cell lines, as evaluated by real-time quantitative reverse transcriptase PCR. Results are presented as expression levels of each gene relative to a reference gene (*GAPDH*) to correct for variations in the amount of RNA. Five of the 10 genes (left: *C1orf77*, *SNAPAP*, *INTS3*, *CRTX2*, and *CREB3L4*) were overexpressed in SNU368 cells; the other 5 genes were not overexpressed (right: *S100A6*, *S100A2*, *S100A16*, *GATAD2B*, and *JTB*).

3.3. Identification of candidate target genes in 1q21 amplicon

To explore candidate target genes involved in 1q21 amplification, we determined the expression levels of all 26 genes within the amplicon in our panel of 19 HCC cell lines by real-time quantitative reverse transcriptase PCR. Five genes (*C1orf77*, *SNAPAP*, *INTS3*, *CRTC2*, and *CREB3L4*) were found to be overexpressed in SNU368 cells showing amplification at 1q21, as shown in Figure 3. In several other lines, one or more of those five genes was overexpressed without amplification. These findings suggested that the five genes are candidate targets for 1q21 amplification.

3.4. Upregulated expression of *CREB3L4*, *INTS3*, and *SNAPAP* in primary HCC tumors

We determined the expression levels of the five candidate genes in paired tumor and nontumor tissues from 18 HCC patients using real-time quantitative reverse transcriptase PCR. *CREB3L4*, *INTS3*, and *SNAPAP* were significantly overexpressed in 14 (78%), 14 (78%), and 13 (72%) of the tumors, respectively, compared with their counterpart nontumorous tissues (Wilcoxon signed-rank test; $P = 0.006$, $P = 0.015$, and $P = 0.014$, respectively) (Fig. 4). On the other hand, expression of *C1orf77* or *CRTC2* was not upregulated in HCC tumors. These results suggest that *CREB3L4*, *INTS3*, and *SNAPAP* are probable target for the 1q21 amplicon.

4. Discussion

The high-density SNP array analysis successfully identified high-level amplification in the narrow region at 1q21 in HCC cell lines (Figs. 1A, 1B). Frequent amplification in this region has been observed not only in HCC cell lines but also in primary HCC tumors (Figs. 1D, 2). Possible oncogenes such as *ETV3* (alias *PE-1*) [34], *MUC1* [35], and *NTRK1* (alias *TRK*) [36] are located within 1q21. Three growth-related genes located in 1q21, *HAX1*, *SHC1*, and *CKS1B*, were shown to be upregulated in HCC tumors, compared with the nontumorous tissues [37]; however, the positions of these genes were outside the amplicon we detected. The results of subsequent experiments suggest that *CREB3L4*, *INTS3*, and *SNAPAP* are probable targets for the amplicon among the 26 genes examined; the three transcripts were overexpressed in SNU368 cells that exhibited amplification (Fig. 3) and were significantly upregulated in primary HCC tumors, compared with their nontumorous counterparts (Fig. 4).

CREB3L4 (cyclic AMP responsive element protein 3-like 4), also referred to as *AlbZIP* [38], belongs to the CREB/ATF family of transcriptional factors. In humans, *CREB3L4* transcripts are detected exclusively in the prostate, as well as in prostate and breast cancer cell lines [38]. Immunostaining of prostate tumors showed that *CREB3L4* protein levels were higher in cancerous prostate cells than in adjacent noncancerous cells [38]. *INTS3*

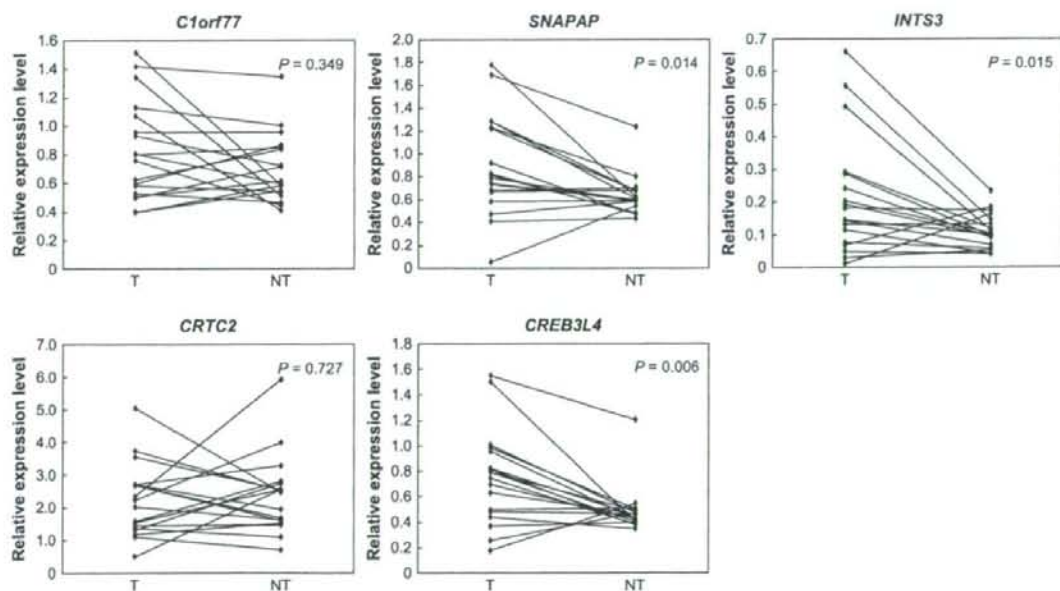


Fig. 4. Relative expression of *C1orf77*, *SNAPAP*, *INTS3*, *CRTC2*, and *CREB3L4* in paired tumor (T) and nontumor tissues (NT) from 18 patients with primary HCC. *CREB3L4*, *INTS3*, and *SNAPAP* were significantly overexpressed in primary HCC tumors. Expression levels of each gene were evaluated by real-time quantitative reverse transcriptase PCR and normalized against levels of *GAPDH*.

(integrator complex subunit 3) encodes one of the subunits of the Integrator complex. Baillat et al. [39] described an RNA polymerase II complex that contains at least 12 novel subunits, termed the Integrator, in addition to core RNA polymerase II subunits. The Integrator is found to be associated with the C-terminal domain of RNA polymerase II and mediates the processing of small nuclear RNAs (snRNAs). SNAPAP (snare-associated protein; also known as Snapin), is a component of the SNARE complex of proteins that is implicated in synaptic vesicle docking and fusion [40], and is also a component of biogenesis of lysosome-related organelles complex-1 (BLOC-1), a ubiquitously expressed multisubunit protein complex required for the normal biogenesis of specialized organelles of the endosomal-lysosomal system [41]. Little is known about the possible relationships between *INTS3* or *SNAPAP* and tumorigenesis.

Functional studies are needed to clarify the roles of these three genes in 1q21 amplification, because it is possible that coactivation of these genes leads to development and progression not only of HCCs but also of other types of tumors.

Acknowledgments

This work was supported by Grants-in-Aid for Scientific Research from the Japan Society for the Program of Science to K.Y. and T.O.

References

- [1] Kallioniemi A, Kallioniemi OP, Sudar D, Rutovitz D, Gray JW, Waldman F, Pinkel D. Comparative genomic hybridization for molecular cytogenetic analysis of solid tumors. *Science* 1992;258:818–21.
- [2] Yasui K, Arai S, Zhao C, Imoto I, Ueda M, Nagai H, Emi M, Inazawa J. TFD1, CUL4A, and CDC16 identified as targets for amplification at 13q34 in hepatocellular carcinomas. *Hepatology* 2002; 35:1476–84.
- [3] Okamoto H, Yasui K, Zhao C, Arai S, Inazawa J. *PTK2* and *EIF3S3* genes may be amplification targets at 8q23-q24 and are associated with large hepatocellular carcinomas. *Hepatology* 2003;38:1242–9.
- [4] Fukuda Y, Kurihara N, Imoto I, Yasui K, Yoshida M, Yanagihara K, Park JG, Nakamura Y, Inazawa J. *CD44* is a potential target of amplification within the 11p13 amplicon detected in gastric cancer cell lines. *Genes Chromosomes Cancer* 2000;29:315–24.
- [5] Yokoi S, Yasui K, Saito-Ohara F, Koshikawa K, Iizasa T, Fujisawa T, Terasaki T, Horii A, Takahashi T, Hirohashi S, Inazawa J. A novel target gene, *SKP2*, within the 5p13 amplicon that is frequently detected in small cell lung cancers. *Am J Pathol* 2002;161:207–16.
- [6] Yokoi S, Yasui K, Iizasa T, Imoto I, Fujisawa T, Inazawa J. *TERC* identified as a probable target within the 3q26 amplicon that is detected frequently in non-small cell lung cancers. *Clin Cancer Res* 2003;9:4705–13.
- [7] Mei R, Galipeau PC, Prass C, Berno A, Ghandour G, Patil N, Wolff RK, Chee MS, Reid BJ, Lockhart DJ. Genome-wide detection of allelic imbalance using human SNPs and high-density DNA arrays. *Genome Res* 2000;10:1126–37.
- [8] Matsuzaki H, Loi H, Dong S, Tsai YY, Fang J, Law J, Di X, Liu WM, Yang G, Liu G, Huang J, Kennedy GC, Ryder TB, Marcus GA, Walsh PS, Shriver MD, Puck JM, Jones KW, Mei R. Parallel genotyping of over 10,000 SNPs using a one-primer assay on a high-density oligonucleotide array. *Genome Res* 2004;14:414–25. [Erratum in: *Genome Res* 2004;14:786].
- [9] Zhao X, Li C, Paez JG, Chin K, Janne PA, Chen TH, Girard L, Minna J, Christiani D, Leo C, Gray JW, Sellers WR, Meyerson M. An integrated view of copy number and allelic alterations in the cancer genome using single nucleotide polymorphism arrays. *Cancer Res* 2004;64:3060–71.
- [10] Bignell GR, Huang J, Greshock J, Watt S, Butler A, West S, Grigorova M, Jones KW, Wei W, Stratton MR, Futreal PA, Weber B, Shaper MH, Wooster R. High-resolution analysis of DNA copy number using oligonucleotide microarrays. *Genome Res* 2004;14:287–95.
- [11] Wong KK, Tsang YT, Shen J, Cheng RS, Chang YM, Man TK, Lau CC. Allelic imbalance analysis by high-density single-nucleotide polymorphic allele (SNP) array with whole genome amplified DNA. *Nucleic Acids Res* 2004;32:e69.
- [12] Matsuzaki H, Dong S, Loi H, Di X, Liu G, Hubbell E, Law J, Bernsten T, Chadha M, Hui H, Yang G, Kennedy GC, Webster TA, Cawley S, Walsh PS, Jones KW, Fodor SP, Mei R. Genotyping over 100,000 SNPs on a pair of oligonucleotide arrays. *Nat Methods* 2004;1:109–11.
- [13] Garraway LA, Widlund HR, Rubin MA, Getz G. Integrative genomic analyses identify *MET* as a lineage survival oncogene amplified in malignant melanoma. *Nature* 2005;436:117–22.
- [14] Zhao X, Weir BA, LaFramboise T, Lin M, Beroukhim R, Garraway L, Beheshti J, Lee JC, Naoki K, Richards WG, Sugarbaker D, Chen F, Rubin MA, Janne PA, Girard L, Minna J, Christiani D, Li C, Sellers WR, Meyerson M. Homozygous deletions and chromosome amplifications in human lung carcinomas revealed by single nucleotide polymorphism array analysis. *Cancer Res* 2005;65:5561–70.
- [15] Bosch FX, Ribes J, Cléries R, Díaz M. Epidemiology of hepatocellular carcinoma. *Clin Liver Dis* 2005;9:191–211.
- [16] Marchio A, Meddeb M, Pineau P, Danglot G, Tiollais P, Bernheim A, Dejean A. Recurrent chromosomal abnormalities in hepatocellular carcinoma detected by comparative genomic hybridization. *Genes Chromosomes Cancer* 1997;18:59–65.
- [17] Kusano N, Shiraiishi K, Kubo K, Oga A, Okita K, Sasaki K. Genetic aberrations detected by comparative genomic hybridization in hepatocellular carcinomas: their relationship to clinicopathological features. *Hepatology* 1999;29:1858–62.
- [18] Guan XY, Fang Y, Sham JS, Kwong DL, Zhang Y, Liang Q, Li H, Zhou H, Trent JM. Recurrent chromosome alterations in hepatocellular carcinoma detected by comparative genomic hybridization. *Genes Chromosomes Cancer* 2000;29:110–6.
- [19] Poon TC, Wong N, Lai PB, Rattray M, Johnson PJ, Sung JJ. A tumor progression model for hepatocellular carcinoma: bioinformatic analysis of genomic data. *Gastroenterology* 2006;131:1262–70.
- [20] Knuutila S, Björkqvist AM, Autio K, Tarkkanen M, Wolf M, Monni O, Szymanska J, Larramendy ML, Tapper J, Pere H, El-Rifai W, Hemmer S, Wasenius VM, Vidgren V, Zhu Y. DNA copy number amplifications in human neoplasms: review of comparative genomic hybridization studies. *Am J Pathol* 1998;152:1107–23.
- [21] Larramendy ML, Virolainen M, Tukiainen E, Elomaa I, Knuutila S. Chromosome band 1q21 is recurrently gained in desmoid tumors. *Genes Chromosomes Cancer* 1998;23:183–6.
- [22] Dor I, Namba M, Sato J. Establishment and some biological characteristics of human hepatoma cell lines. *Gann* 1975;66:385–92.
- [23] Alexander JJ, Bey EM, Geddes EW, Lecatsas G. Establishment of a continuously growing cell line from primary carcinoma of the liver. *S Afr Med J* 1976;50:2124–8.
- [24] Hirohashi S, Shimosato Y, Kameya T, Koide T, Mukojima T, Taguchi Y, Kageyama K. Production of alpha-fetoprotein and normal serum proteins by xenotransplanted human hepatomas in relation to their growth and morphology. *Cancer Res* 1979;39:1819–28.

- [25] Nakabayashi H, Taketa K, Miyano K, Yamane T, Sato J. Growth of human hepatoma cells lines with differentiated functions in chemically defined medium. *Cancer Res* 1982;42:3858–63.
- [26] Aden DP, Fogel A, Plotkin S, Damjanov I, Knowles BB. Controlled synthesis of HBsAg in a differentiated human liver carcinoma-derived cell line. *Nature* 1979;282:615–6.
- [27] Park JG, Lee JH, Kang MS, Park KJ, Jeon YM, Lee HJ, Kwon HS, Park HS, Yeo KS, Lee KU. Characterization of cell lines established from human hepatocellular carcinoma. *Int J Cancer* 1995;62:276–82.
- [28] Fujise K, Nagamori S, Hasumura S, Homma S, Sujino H, Matsuura T, Shimizu K, Niiya M, Kameda H, Fujita K. Integration of hepatitis B virus DNA into cells of six established human hepatocellular carcinoma cell lines. *Hepatogastroenterology* 1990;37:457–60.
- [29] Huh N, Utakoji T. Production of HBs-antigen by two new human hepatoma cell lines and its enhancement by dexamethasone. *Gann* 1981;72:178–9.
- [30] Kennedy GC, Matsuzaki H, Dong S, Liu WM, Huang J, Liu G, Su X, Cao M, Chen W, Zhang J, Liu W, Yang G, Di X, Ryder T, He Z, Surti U, Phillips MS, Boyce-Jacino MT, Fodor SP, Jones KW. Large-scale genotyping of complex DNA. *Nat Biotechnol* 2003;21:1233–7.
- [31] Di X, Matsuzaki H, Webster TA, Hubbell E, Liu G, Dong S, Bartell D, Huang J, Chiles R, Yang G, Shen MM, Kulp D, Kennedy GC, Mei R, Jones KW, Cawley S. Dynamic model based algorithms for screening and genotyping over 100 K SNPs on oligonucleotide microarrays. *Bioinformatics* 2005;21:1958–63.
- [32] Huang J, Wei W, Zhang J, Liu G, Bignell GR, Stratton MR, Futreal PA, Wooster R, Jones KW, Shaper MH. Whole genome DNA copy number changes identified by high density oligonucleotide arrays. *Hum Genomics* 2004;1:287–99.
- [33] Minamiya Y, Matsuzaki I, Sageshima M, Saito H, Taguchi K, Nakagawa T, Ogawa J. Expression of tissue factor mRNA and invasion of blood vessels by tumor cells in non-small cell lung cancer. *Surg Today* 2004;34:1–5.
- [34] Klemsz M, Hromas R, Raskind W, Bruno E, Hoffman R. PE-1, a novel ETS oncogene family member, localizes to chromosome 1q21-q23. *Genomics* 1994;20:291–4.
- [35] Denda-Nagai K, Irimura T. MUC1 in carcinoma-host interactions. *Glycoconj J* 2000;17:649–58.
- [36] Bongarzone I, Pierotti MA, Monzini N, Mondellini P, Manenti G, Donghi R, Pilotti S, Grieco M, Santoro M, Fusco A. High frequency of activation of tyrosine kinase oncogenes in human papillary thyroid carcinoma. *Oncogene* 1989;4:1457–62.
- [37] Midorikawa Y, Tsutsumi S, Nishimura K, Kamimura N, Kano M, Sakamoto H, Makuuchi M, Aburatani H. Distinct chromosomal bias of gene expression signatures in the progression of hepatocellular carcinoma. *Cancer Res* 2004;64:7263–70.
- [38] Qi H, Fillion C, Labrie Y, Grenier J, Fournier A, Berger L, El-Alfy M, Labrie C. AlBZIP, a novel bZIP gene located on chromosome 1q21.3 that is highly expressed in prostate tumors and of which the expression is upregulated by androgens in LNCaP human prostate cancer cells. *Cancer Res* 2002;62:721–33.
- [39] Baillat D, Hakimi MA, Naar AM, Shilatfard A, Cooch N, Shiekhhattar R. Integrator, a multiprotein mediator of small nuclear RNA processing, associates with the C-terminal repeat of RNA polymerase II. *Cell* 2005;123:265–76.
- [40] Ilardi JM, Mochida S, Sheng ZH. Snapin: a SNARE-associated protein implicated in synaptic transmission. *Nat Neurosci* 1999;2:119–24.
- [41] Starcevic M, Dell'Angelica EC. Identification of snapin and three novel proteins (BLOS1, BLOS2, and BLOS3/reduced pigmentation) as subunits of biogenesis of lysosome-related organelles complex-1 (BLOC-1). *J Biol Chem* 2004;279:28393–401.

Review

Adipocytokines and liver disease

YOSHIHIRO KAMADA, TETSUO TAKEHARA, and NORIO HAYASHI

Department of Gastroenterology and Hepatology, Osaka University, Graduate School of Medicine, 2-2 K1 Yamadaoka, Suita, Osaka 565-0871, Japan

Adipose tissue is a massive source of bioactive substances known as adipocytokines, including tumor necrosis factor (TNF)- α , resistin, leptin, and adiponectin. Recent advances in medical research view obesity as a chronic low-grade inflammatory state. Hypertrophied adipocytes in obesity release chemokines that induce macrophage accumulation in adipose tissue. Accumulated macrophages in obese adipose tissue produce proinflammatory cytokines and nitric oxide, and these inflammatory changes induce adipocytokine dysregulation. The latter is characterized by a decrease in insulin-sensitizing and anti-inflammatory adipocytokines, and an increase in proinflammatory adipocytokines. Adipocytokine dysregulation induces obesity-related metabolic disorders, the so-called metabolic syndrome. Metabolic syndrome is a cluster of metabolic abnormalities, including diabetes mellitus, hypertension, hyperlipidemia, and nonalcoholic steatohepatitis (NASH). Recent studies have revealed that obesity is an independent risk factor for chronic liver diseases, such as NASH, alcoholic liver disease, chronic hepatitis C, and hepatocellular carcinoma. A common mechanism underlying these hepatic clinical states is thought to be adipocytokine dysregulation. In this review, we discuss the association of adipocytokines, especially leptin, adiponectin, TNF- α , and resistin, with liver diseases.

Key words: nonalcoholic steatohepatitis (NASH), chronic hepatitis C, obesity, adipocytokine, adiponectin, leptin, TNF- α

Introduction

Adipose tissue is an energy-storing organ that produces and secretes several bioactive substances^{1,2} known as

adipocytokines,³ such as adiponectin,⁴ leptin,⁵ resistin,⁶ plasminogen activator inhibitor 1 (PAI-1),³ and tumor necrosis factor α (TNF- α).⁷ Recent studies have suggested that obesity is a state of chronic, low-grade inflammation that contributes to insulin resistance and type 2 diabetes.^{8,9} Hypertrophied adipocytes in obesity release chemokines, which recruit macrophages, especially in visceral adipose tissue. Adipose tissue macrophages produce nitric oxide (NO) and inflammatory cytokines such as TNF- α , interleukin (IL)-6, and IL-1 β . These inflammatory changes in adipose tissue induce adipocytokine dysregulation: a decrease in insulin-sensitizing and anti-inflammatory adipocytokines such as adiponectin, and an increase in proinflammatory adipocytokines involved in insulin resistance such as TNF- α , interleukins, and resistin^{10,11} (Fig. 1). Furthermore, adipocytokine dysregulation is thought to play a crucial role in metabolic syndrome.¹²

Hepatic cirrhosis is six times more prevalent in obese individuals than in the general population,^{13,14} and obesity is an independent risk factor for severity of liver fibrosis in nonalcoholic steatohepatitis (NASH), alcohol-induced liver disease, chronic hepatitis C (CHC), and hepatocellular carcinoma (HCC).^{14–20} Recently, several studies have reported that adipocytokine dysregulation affects the pathological state of liver diseases.^{21–24} For example, serum leptin and TNF- α levels were significantly higher, and adiponectin levels were significantly lower, in patients with NASH than in controls.²² In this review, we describe the important roles of adipocytokines in liver diseases.

Leptin

Leptin is a 167-amino acid secreted protein encoded by the *ob* gene, and was identified by positional cloning in the *ob/ob* mouse as a key molecule in the regulation of body weight and energy balance.²⁵ Leptin is produced

Received / Accepted: May 1, 2008
Reprint requests to: N. Hayashi

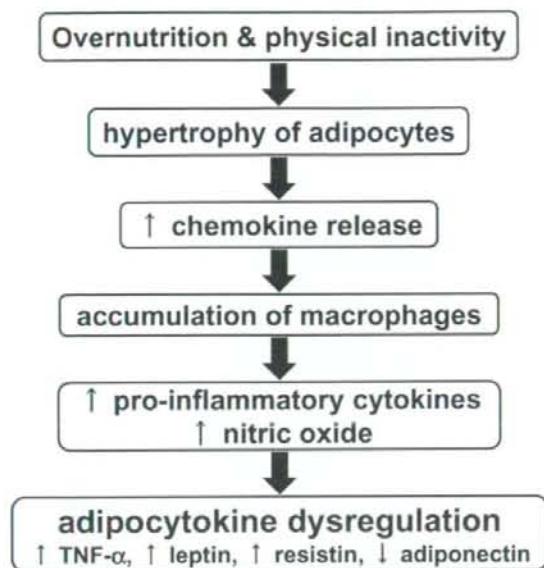


Fig. 1. Current hypothesis regarding the mechanism of adipocytokine dysregulation. *TNF- α* , tumor necrosis factor α

mainly by adipocytes. The expression of leptin in adipocytes is transcriptionally regulated, and is determined mainly by the status of energy stores in white adipose tissue and the size of adipocytes.⁵ However, recent studies have confirmed that leptin is also expressed in other tissues such as skeletal muscles, stomach, ovaries, and liver.³⁶ Leptin plays a key role in the regulation of appetite and body weight. It also acts on the hypothalamus, altering energy intake by decreasing appetite and increasing energy expenditure via sympathetic stimulation of several tissues.³⁷ Mutations in the leptin gene cause obesity in rodents and human.^{35,38}

Serum leptin concentrations correlate well with body weight and body fat mass, and are higher in women than in men even after adjustment for age and body mass index.³⁹

Leptin resistance

Circulating leptin levels are elevated in obese subjects, but these subjects are resistant to the action of leptin. Leptin acts by binding to its receptor, Ob-R, and its gene is alternatively spliced into several isoforms. One of the splice variants, Ob-Re, is a soluble leptin receptor and binds to leptin to form a leptin-Ob-Re complex.⁴⁰ The complex formation can delay leptin clearance and thereby increase the availability of bioactive leptin.⁴¹ In obese individuals, the serum free leptin level is high, and the Ob-Re level is low, resulting in a low leptin-Ob-Re complex level. A low serum Ob-Re level and low

leptin-Ob-Re complex level can be markers of leptin resistance. However, excess Ob-Re is likely to inhibit free leptin function, because the complex cannot activate the transmembrane leptin receptor Ob-Rb.⁴⁰ Other groups have argued that diet-induced obesity causes downregulation of Ob-Rb and results in impairment of leptin signaling.^{42,43}

Recent studies indicate that leptin can inhibit the orexigenic peptides (neuropeptide Y, agouti-related peptide) and stimulate the secretion of anorexigenic peptide (α -melanocyte-stimulating hormone) from arcuate melanocortin neurons of lean mice.⁴⁴ However, leptin failed to modulate the secretion of these peptides in high-fat-diet-induced obese (DIO) mice. Such resistance to leptin is due to increased levels of suppressor of cytokine-signaling protein 3 (a negative regulator of leptin signal transduction) in the arcuate nucleus in the hypothalamus of DIO mice. A reduction in diet fat content resulted in recovery of leptin responsiveness in DIO mice.

Leptin and liver diseases

In animal models, leptin prevents lipid accumulation in nonadipose tissues, such as skeletal muscles, pancreas, and liver, a concept referred to as lipotoxicity.²³ In the liver, leptin achieves its antilipogenic effects by lowering the expression of sterol regulatory element binding protein 1 (SREBP-1).⁴⁵ Patients with severe lipodystrophy present with hepatic steatosis and hepatocellular ballooning injury, similar to that seen in NASH, and recombinant leptin significantly reduces serum levels of triglycerides, transaminases, and liver fat content and improves hepatomegaly in these patients.⁴⁶

Leptin injections in mice treated with carbon tetrachloride increased the expression levels of procollagen-I, transforming growth factor β 1 (TGF- β 1), and smooth muscle actin, a marker of activated hepatic stellate cells (HSCs), and eventually resulted in tissue fibrosis.⁴⁷ In the liver, leptin directly promotes fibrogenesis by stimulating the production of tissue inhibitor of metalloproteinase 1 via the Janus kinase/signal transducer and activator of transcription pathway in activated HSCs, which are a central player in liver fibrosis.⁴⁸ Moreover, leptin is described as a potent mitogen for HSCs and an inhibitor of apoptosis of HSCs through extracellular signal-regulated kinase (ERK) and the Akt-dependent pathway.⁴⁹ Activated HSCs acquire the ability of secrete leptin and are thought to further promote liver fibrosis.⁵⁰ In addition, leptin increases the expression of TGF- β 1 in sinusoidal endothelial cells and Kupffer cells. In Zucker (*fa/fa*) rats, a naturally occurring functional leptin receptor-deficient animal, thioacetamide-induced hepatic fibrosis was prevented almost completely and induction of TGF- β 1 and activation of HSCs were

abolished.⁵⁰ Considered together, the above results indicate that leptin and its functional receptor play a pivotal role in profibrogenic responses in the liver.

High serum leptin concentrations are present in cirrhosis patients.^{30,34} However, despite high serum leptin concentrations in nonalcoholic fatty liver disease (NAFLD) patients, there is no relationship between leptin and the severity of hepatic fibrosis.⁵¹ Moreover, leptin levels were initially found to be significantly higher in NASH patients than in controls matched for sex and body mass index (BMI), and correlated with the severity of hepatic steatosis but not with the severity of inflammation or fibrosis.²³ In another study, serum leptin levels and leptin receptor mRNA expression levels in the liver were not significantly different between patients with NASH and those with simple steatosis.⁵² The relationship between serum leptin concentrations and the severity of liver fibrosis remains to be investigated.

Serum leptin levels were higher in CHC patients than controls,⁵³ and associated with the severity of fibrosis.⁵⁴ Serum leptin levels correlated with hepatic steatosis in patients infected with hepatitis C virus genotype 3 but not genotype 1.⁵⁵ In contrast, another study revealed that leptin levels do not correlate with fibrosis or severity of steatosis in CHC patients.⁵⁶ Considered together, these studies indicate that while serum leptin levels may be elevated in CHC patients, there is rather a conflicting relationship between serum leptin levels and liver histology in such patients.

There is a close relationship between BMI and a high mortality rate due to digestive cancers;¹⁹ especially, obesity and HCC represent a particularly high risk.^{20,57} The high plasma leptin levels in obesity may contribute to this phenomenon. Leptin acts as mitogen on many cell types *in vitro*, including HCC cells, via the ERK/mitogen-activated protein kinase (MAPK), and phosphatidylinositol 3-kinase (PI3K)/Akt pathway, and may facilitate progression to liver cancer *in vivo*.^{58,59}

These findings suggest that leptin plays important roles in liver diseases such as attenuating hepatic steatosis, exacerbating liver fibrosis, and possibly promoting HCC growth. Further research needs to be conducted on the precise role of leptin in liver diseases.

Adiponectin

Adiponectin is an adipocyte-specific 28-kDa secreted protein expressed exclusively in adipose tissue.⁴ However, recent studies have indicated that adiponectin is also produced by organs other than adipose tissue, such as bone marrow,⁶⁰ fetal tissue,⁶¹ cardiomyocytes,⁶² and hepatic endothelial cells.^{31,63} However, the major source of plasma adiponectin in adults is adipocytes.

The protein contains a signal sequence and a collagen-repeat domain at the N terminus, and a C1q-like globular domain at the C terminus.⁶⁴ Adiponectin is present in a wide range of multimer complexes in plasma and assembles via its collagen domain into adiponectin trimers (low molecular weight), hexamers (middle molecular weight), and 12- to 18-mers [high molecular weight (HMW)].⁶⁴⁻⁶⁶ The HMW forms appear to be responsible for insulin sensitivity and the anti-inflammatory effects of adiponectin.^{65,67} Hydroxylation and glycosylation of the lysine residues within the collagen domain are critically involved in the regulation of HMW adiponectin formation.⁶⁸ The full-length adiponectin protein is proteolytically cleaved, with a smaller form including the globular domain, although in very small amounts.⁶⁹

Adiponectin protein is present at high levels (range, 3–30 µg/ml) in plasma, accounting for about 0.01% of total plasma protein. Surprisingly, the plasma adiponectin level is inversely correlated with BMI in spite of its restricted expression in adipose tissue.⁶⁶ Especially, the plasma adiponectin level is low in subjects with visceral fat accumulation. Hypoadiponectinemia has been demonstrated to be independently associated with metabolic syndrome, including type 2 diabetes,⁷⁰ hypertension,⁷¹ atherosclerosis,⁷² and NASH.²⁵ Weight reduction results in a significant elevation of plasma adiponectin levels in humans.⁷⁰

Why are plasma adiponectin levels low in obese subjects? While the exact mechanism is unknown, several theories have been postulated. TNF- α , one of the insulin resistance inducible factors, is upregulated in obese subjects, and suppresses the expression and plasma levels of adiponectin at the transcriptional level.⁷² Production of reactive oxygen species (ROS) is selectively increased in adipose tissue of obese mice, accompanied by augmented expression of NADPH oxidase. Production of adiponectin is downregulated by elevated oxidative stress in adipose tissue. NADPH oxidase inhibitor reduces ROS production and increases adiponectin production in adipose tissue.⁷³ The frequency of a missense mutation at position 164 in the globular domain [Ile-164The (I164T)] is significantly higher in patients with type 2 diabetes and coronary artery disease than in normal control subjects.^{74,75} Subjects with this mutation had significantly lower plasma adiponectin levels than those without it.

Adiponectin receptor

Two receptors for adiponectin, AdipoR1 and AdipoR2, have been cloned.⁷⁶ These adiponectin receptors are considered to contain seven transmembrane domains, despite being structurally and functionally distinct from G protein-coupled receptors. AdipoR1 is ubiquitously

expressed and is abundantly expressed in skeletal muscle, whereas AdipoR2 is most abundantly expressed in the liver. AdipoR1 and AdipoR2 serve as receptors for globular and full-length adiponectin and activate adenosine monophosphate-activated protein kinase (AMPK), peroxisome proliferator-activated receptor- α (PPAR- α), and p38 MAPK signaling pathways.⁷⁷ Disruption of these receptors abolished adiponectin binding and its actions.⁷⁸ Insulin reduces the expression of AdipoR1 and AdipoR2 via a PI3K/Forkhead boxO1-dependent pathway in cultured hepatocytes or myocytes.^{28,79}

T-cadherin serves as a receptor for the hexameric and HMW forms of adiponectin.⁸⁰ Because T-cadherin is a glycosylphosphatidylinositol-anchored extracellular protein, it may act as a coreceptor for an unidentified signaling receptor.

Adiponectin and NAFLD

Obesity is an independent risk factor in the development of NASH²¹⁻²³ and HCC,^{19,34} and patients with NASH who progress to liver cirrhosis are at increased risk of HCC.⁸¹ In the two-hit theory of NASH pathogenesis, the first hit of hepatic steatosis is followed by the second hit of oxidative injury, leading to inflammation and progression to fibrosis and HCC.^{81,82} In the following paragraphs, we focus on the roles of adiponectin in the two-hit theory of NASH pathogenesis.

Adiponectin and hepatic steatosis

We found that hepatic steatosis, induced by a choline-deficient L-amino acid-defined (CDAA) diet, is more severe in adiponectin knockout mice than in wild-type mice.⁸³ The CDAA diet was used to induce a nutritional animal model of NASH.⁸⁴ Overexpression of adiponectin protein by adenovirus vector resulted in attenuation of hepatic steatosis. The lack of adiponectin in these mice enhanced the expression of two rate-limiting enzymes in fatty acid synthesis, acetyl-CoA carboxylase (ACC) and fatty acid synthase. Adiponectin is also known to stimulate mitochondrial β -oxidation by activation of AMPK and PPAR- α .^{65,69} Activated PPAR- α upregulates carnitine palmitoyltransferase (CPT)-1, a rate-limiting enzyme in fatty acid oxidation. In addition, activated AMPK phosphorylates ACC and attenuates the activity of ACC. Inactivation of ACC leads to a decrease in the concentration of its product, malonyl-CoA (a potent inhibitor of CPT-1), and induces fatty acid oxidation in the liver. Moreover, adiponectin downregulates SREBP-1c, a master regulator of fatty acid synthesis.⁸⁵ Thus, adiponectin increases β -oxidation of free fatty acids and decreases de novo free fatty acids production within hepatocytes.^{69,86} These effects protect hepatocytes against triglyceride accumulation. The

hypoadiponectinemia in obese individuals could exacerbate hepatic steatosis, the first hit in NASH, through the absence of these effects of adiponectin.

Adiponectin and inflammation

Adiponectin at physiological concentrations attenuates the attachment of monocytes to endothelial cells by reducing TNF- α -induced expression of adhesion molecules such as vascular cell adhesion molecule 1, endothelial-leukocyte adhesion molecule-1 (E-selectin), and intercellular cell adhesion molecule 1.⁷² Nuclear transcription factor, nuclear factor κ B (NF κ B), induces the expression of cytokines and adhesion molecules in the inflammatory process. Adiponectin suppresses TNF- α -induced NF κ B activation and blocks TNF- α release in endothelial cells.⁸⁷

C-reactive protein (CRP) is a potent marker of systemic inflammation, and its plasma level correlates negatively and significantly with adiponectin levels in humans.^{88,89} CRP levels correlate with body weight and percentage of body fat,⁹⁰ and CRP mRNA is expressed in human adipose tissue and its levels correlate inversely with adiponectin gene expression in human adipose tissue.⁸⁸

Patients with NASH are at increased risk of small intestinal bacterial overgrowth,⁹¹ and lipopolysaccharide (LPS) is involved in the pathogenesis of NASH.^{92,93} In a mouse model of LPS-induced acute hepatitis, we found that adiponectin protected against hepatic injury through inhibition of production of the proinflammatory cytokine TNF- α and induction of the anti-inflammatory cytokine IL-10 in Kupffer cells.⁹⁴ Lack of adiponectin accelerated LPS-induced liver injury, and the survival rate of adiponectin knockout mice after LPS administration was significantly lower than that of wild-type mice. Pretreatment of these mice with adiponectin reduced LPS-induced TNF- α production, and increased IL-10 production by Kupffer cells. These findings are in agreement with another study in which pretreatment of KK-Ay obese mice with adiponectin protected them from LPS-induced hepatic injury through modulation of TNF- α .⁹⁵ Other investigators have shown that adiponectin also suppresses macrophage function⁹⁶ and induces anti-inflammatory cytokines, such as IL-10 and IL-1RA, in human leukocytes.^{97,98} In addition, adiponectin alleviates experimental T-cell-mediated hepatitis induced by concanavalin A in mice, and protects primary hepatocytes from TNF- α -induced death.⁹⁹ These results suggest that hypoadiponectinemia in obese subjects can thus lead to enhanced sensitivity of Kupffer cells to proinflammatory mediators such as LPS.

A recent study reported that adiponectin promotes clearance of early apoptotic cells by macrophages through a receptor-dependent pathway involving calre-

ticulin.¹⁰⁰ This novel function of adiponectin is similar to that of surfactant proteins and C1q, which serve as anti-inflammatory molecules by promoting the clearance of apoptotic cell debris.¹⁰¹

Adiponectin and oxidative stress

Obesity is regarded as a chronic inflammatory state. The associated hepatic lipid overload induces impairment of mitochondrial β oxidation, which may lead to the formation of ROS and lipid peroxidation products. ROS and lipid peroxidation in turn upregulate a series of proinflammatory cytokines,¹⁰² causing further mitochondrial dysfunction and oxidative stress, thus contributing to the progression of liver injury.

Recent studies indicate that adiponectin can suppress oxidative stress,^{103,104} and that systemic oxidative stress, as measured by urinary 8-epi-prostaglandin F_{2 α} , correlates strongly with hypo adiponectinemia.¹⁰⁵ Studies from our laboratories showed enhanced oxidative stress in adiponectin knockout mice in a CDAA diet-induced NASH mouse model.⁸³ Accumulating evidence suggests that alcohol-mediated upregulation of CYP2E1 may initiate lipid peroxidation via production of ROS.¹⁰⁶ CYP2E1 is upregulated in human liver in NASH,¹⁰⁷ and in a rodent model of NASH.^{108,109} In our CDAA diet-induced NASH mouse model, CYP2E1 was induced in adiponectin knockout mice and adiponectin overexpression downregulated CYP2E1.⁸³ Moreover, thiobarbituric acid reactive substance, a marker of oxidative stress, and 8-hydroxydeoxyguanosine, a marker of oxidative DNA damage, were also increased in the livers of adiponectin knockout mice. Adiponectin knockout mice also showed significantly enhanced hepatic tumor formation compared with wild-type mice. Thus, adiponectin deficiency might enhance the level of oxidative stress through induction of CYP2E1 in the liver, allowing progression of liver injury in adiponectin-deficient mice.

TNF- α plays crucial roles in NASH progression,^{110,111} and adiponectin suppresses TNF- α production.⁹⁶ In our study, we found significantly elevated serum levels of TNF- α in adiponectin knockout mice,⁸³ which may play a role in the progression of hepatopathology in adiponectin knockout mouse liver.

Adiponectin and fibrosis

In a clinical study of NASH patients, the fibrosis stage correlated significantly with low serum adiponectin levels.²⁹ We reported previously that adiponectin attenuates carbon tetrachloride-induced liver fibrosis.¹¹² Adiponectin suppressed the proliferation and migration of activated HSCs, which play central roles in liver fibrosis, and attenuated the effect of TGF- β 1 on the expression of fibrogenic genes, and on nuclear translocation of Smad2 in HSCs. Other groups have reported that adi-

ponectin induces apoptosis of activated HSCs,¹¹³ and activated AMPK, which modulates the activated HSC phenotype.^{114,115} These findings indicate that adiponectin has antifibrogenic properties in liver diseases through the suppression of activated HSC proliferation and fibrogenic function.

Inflammation and fibrosis of the liver have recently been reported in individuals with nonalcoholic fatty liver, which is frequently associated with obesity and type-2 diabetes. A considerable number of these patients develop liver cirrhosis, a clinical entity termed NASH. In addition, epidemiological studies have shown that obesity, which is associated with hypo adiponectinemia, is a risk factor for the development of liver fibrosis in patients with NASH, alcoholic liver disease, and CHC.²²⁻³³ These results indicate that hypo adiponectinemia may be one reason obese patients are at high risk for development of liver cirrhosis.

Thus, adiponectin attenuates inflammation, oxidative stress, and proinflammatory cytokine production, which are considered the second hit in NASH. Moreover, adiponectin ameliorates liver fibrosis via suppression of activated HSC function, and might decelerate the progression of hepatocarcinogenesis via suppression of oxidative stress (Fig. 2).

Adiponectin and clinical studies in liver diseases

Adiponectin and NAFLD

In a study of 80 NASH patients, hypo adiponectinemia was independently associated with NASH and with more severe hepatic steatosis and necroinflammation.²⁵ Other reports have also indicated that plasma adiponectin levels are lower in NASH patients than in patients with simple steatosis.^{26,27} Interestingly, the major hepatic adiponectin receptor AdipoR2 is underexpressed in fatty liver and in NASH patients, and *AdipoR2* gene expression correlates inversely with the severity of liver fibrosis.^{27,28} After adjustment for age, sex, and BMI, plasma levels of adiponectin correlated inversely with the alanine transaminase level.⁸⁶ Musso et al.²⁹ reported that hypo adiponectinemia is a feature of NASH and may play a pathogenetic role in hepatic necroinflammation and fibrosis, independent of insulin resistance, visceral fat accumulation, serum TNF- α level, or dietary intake. In contrast, another study demonstrated the presence of hypo adiponectinemia in NAFLD patients but failed to find differences in the serum adiponectin concentration between patients with NASH and those with simple steatosis, and concluded that adiponectin concentration correlated inversely with insulin resistance.¹¹⁶ Considered together, these results suggest that hypo adiponectinemia and underexpression of hepatic adiponectin receptor may play important roles in the clinical progression of NASH.

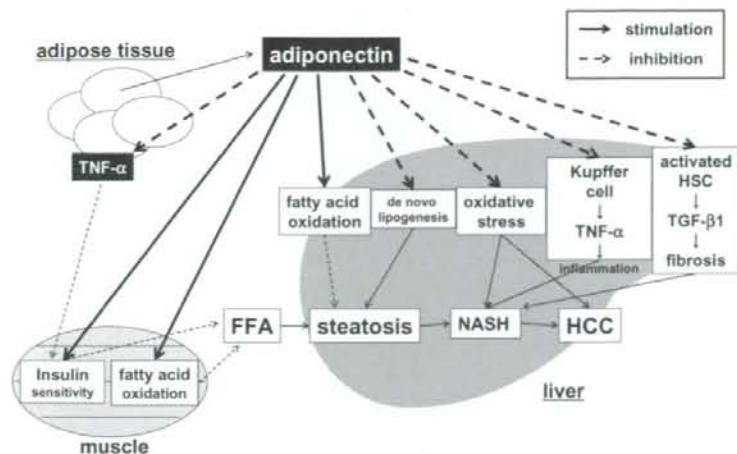


Fig. 2. Roles of adiponectin in NASH development. *Solid arrows*, stimulatory effects; *dotted arrows*, inhibitory effects. *NASH*, nonalcoholic steatohepatitis; *FFA*, free fatty acid; *HCC*, hepatocellular carcinoma; *HSC*, hepatic stellate cell; *TGF-β1*, transforming growth factor β1.

Adiponectin and viral hepatitis

Currently, there is a great interest in the role of adiponectin in CHC. Serum adiponectin levels are higher in CHC patients than in those with chronic hepatitis B.¹¹⁷ In CHC patients, hypoadiponectinemia correlates significantly with steatosis but not with the severity of fibrosis.^{31–33} Hepatic steatosis is a common histological finding in CHC, with an incidence of 305–70%.^{118,119} Hepatic steatosis in CHC correlates with progression of liver fibrosis,^{17,120} and is a risk factor for HCC.¹²¹ In addition, a recent report indicated that low serum adiponectin is an independent predictor of nonvirological response to interferon therapy in CHC patients.³³

On the other hand, hyperadiponectinemia has been described in cirrhosis patients.^{122,123} The liver is the main organ of adiponectin metabolism, and biliary secretion is involved in adiponectin clearance; accordingly, elevated plasma concentrations of adiponectin in advanced cirrhosis are due to decreased metabolism and biliary secretion of adiponectin.

Adiponectin and cancer

Recent studies showed that plasma adiponectin levels are inversely correlated with the risk of cancers.¹²⁴ In clinical studies, hypoadiponectinemia is correlated with colorectal cancer,^{125,126} gastric cancer,¹²⁷ prostate cancer,¹²⁸ endometrial cancer,¹²⁹ and breast cancer.¹³⁰ In addition, *in vitro* studies revealed that adiponectin protein inhibits cell proliferation in cells lines originating from various types of cancer, including prostate cancer, HCC, breast cancer, leukemia, and esophageal cancer.^{96,131–133} These studies emphasize the potential role of hypoadiponectinemia as a risk factor for various cancers.

Pharmacological and dietary interventions

The above findings suggest that hypoadiponectinemia in obese people may be an important risk factor for clinical progression of chronic liver diseases, and that upregulation of adiponectin signaling might be useful therapeutically by increasing plasma adiponectin levels or development of adiponectin receptor agonists. However, considering the high plasma levels of adiponectin, direct administration of adiponectin protein to individuals with liver diseases might not be a good strategy because of difficulties in maintaining high plasma concentrations. Thiazolidinediones elevate the promoter activity of adiponectin and increase the plasma concentration of adiponectin.¹³⁴ Adiponectin promoter has a functional PPAR-responsive element (PPRE) site.¹³⁵ Not only PPARγ but also PPARα ligands increase the expression of adiponectin through a PPRE site located in its promoter region.¹³⁶ Furthermore, PPARα agonist increases the expression of both AdipoR1 and AdipoR2 in adipocytes and macrophages.¹³⁷ Pioglitazone increases the ratio of HMW adiponectin/total adiponectin and increases the hepatic sensitivity to insulin.¹³⁸ These findings indicate that dual activation of PPARγ and PPARα intensifies adiponectin actions by increasing plasma levels of adiponectin, especially HMW adiponectin, and by increasing adiponectin receptors.

Blockade of the renin-angiotensin system (RAS) with angiotensin-converting enzyme inhibitors or angiotensin receptor blocker increases adiponectin concentrations.^{139,140} However, the precise mechanism of increased plasma adiponectin level by RAS blockade remains incompletely unclear.

The effects of diet on plasma adiponectin concentration were recently reported. Dietary soy protein, lin-

oleic acid, and oolong tea increase plasma adiponectin levels in rodents and humans.¹⁴¹⁻¹⁴³ The molecular mechanism of these dietary effects on adiponectin levels remains unclear.

A recent study suggested that osmotin, a member of the PR-5 family of plant defense proteins, is a ligand for the yeast homolog of adiponectin receptor and has functional similarity to adiponectin.¹⁴⁴ Osmotin is abundant in plant tissues (seeds, fruits, vegetables) and is extremely stable; it remains active even when in contact with human digestive or respiratory systems.¹⁴⁴ Further research into similarities in adiponectin and osmotin functions may facilitate the development of potential adiponectin receptor agonists.

Collectively, in addition to weight reduction, the aforementioned pharmacological and dietary interventions can improve hypo adiponectinemia, and might be useful therapeutic approaches to attenuate metabolic syndrome.

TNF- α

TNF- α is a proinflammatory cytokine that was originally found to induce necrosis of tumors after acute bacterial infection. Its first link to obesity, insulin resistance, and chronic inflammation was made in a research paper that described significant elevation of TNF- α in adipose tissue of genetically obese mice (*db/db* mice).¹⁴⁵

The adipose tissue of obese individuals is characterized by increased infiltration of macrophages and hypertrophied adipocytes.¹⁰ Hypertrophied adipocytes release large quantities of free fatty acid (FFA) via macrophage-induced adipocyte lipolysis. FFA serves as a naturally occurring ligand for Toll-like receptor (TLR) 4.^{146,147} FFA increases thereby the production of TNF- α in macrophages through the TLR4/ NF κ B pathway. Thus, a vicious cycle is established.

Kupffer cells are the main producer of TNF- α in the liver, and LPS-induced activation of these cells enhances their production of TNF- α . In animal models, activation of Kupffer cells leads to induction of the TNF- α /TNF receptor signaling pathway, which is critically involved in the pathogenesis of liver fibrosis in NASH.¹¹⁰ In addition, *ob/ob* mice, a model for NAFLD, overexpress TNF- α .⁹² Treatment with anti-TNF antibody reduced the activity of Jun N-terminal kinase, which promotes insulin resistance, and decreased the DNA binding activity of NF κ B, which accelerates inflammation, with a resultant improvement of NAFLD in *ob/ob* mice.

In human, TNF- α levels are increased significantly in simple steatosis and NASH, and correlate with hepatic fibrosis in NASH.²⁶ The gene expression of TNF- α and its receptor are significantly elevated in hepatic and

adipose tissues of NASH patients.²¹ Recently, a histologic scoring system, the NAFLD activity score (NAS), has been proposed that can assist in the diagnosis of NAFLD and may be useful for assessing the response to therapy.¹⁴⁸ Serum TNF- α levels significantly correlated with NAS score.¹⁴⁹ In Japanese NAFLD patients, polymorphisms in the TNF- α promoter region and serum level of soluble TNF receptor 2 significantly correlated with progression of NAFLD.¹⁵⁰ Moreover, administration of pentoxifylline, a TNF- α inhibitor, improved aminotransferase levels and the insulin resistance index assessed by homeostatic metabolic assessment (HOMA-IR) in NASH patients.^{151,152}

Considered collectively, the above data from animal and human studies suggest that TNF- α plays important roles in the progression of NAFLD, including hepatic inflammation and fibrogenesis.

Resistin

Resistin is a member of the resistin-like molecule family of cysteine-rich secretory 12-kDa proteins. In mice, the expression of resistin is restricted to adipose tissue, and the expression of resistin is downregulated by thiazolidinedione and fasting.⁶ Resistin leads to insulin resistance, and hyperresistinemia increases blood glucose and insulin levels in mice.¹⁵³ Resistin overexpression induces dyslipidemia characterized by high serum total cholesterol and triglyceride levels, and reduces high-density lipoprotein cholesterol concentration, which is commonly seen in metabolic syndrome.¹⁵⁴

In humans, resistin expression in adipose tissue is very low, but it is mainly found in bone marrow and in macrophages.^{155,156} Serum resistin concentrations are elevated in patients with NAFLD. Increased resistin levels correlate with histological severity of liver disease but not with insulin resistance.²⁴ Serum resistin levels are higher in obese than in lean individuals, but when adjusted for BMI, resistin levels do not correlate with insulin resistance.¹⁵⁷ The exact role of resistin in obesity and insulin resistance in humans remains elusive. More research is needed to clarify the role of resistin in humans.

Conclusions

We have summarized the recent advances in our understanding of the role of adipocytokines in liver diseases. Adipocytes produce and secrete various adipocytokines to control the functions of other organs, including liver. Production and secretion of adipocytokines are dynamically regulated by nutritional status. Overeating and physical inactivity results in obesity with visceral fat